
APPROXIMATING PERIODIC FUNCTIONS AND SOLVING DIFFERENTIAL EQUATIONS USING A NOVEL TYPE OF FOURIER NEURAL NETWORKS

A PREPRINT

Marieme Ngom

Mathematics and Computer Science division
Argonne National Laboratory
Lemont, IL 60439
mngom@anl.gov

Oana Marin

Mathematics and Computer Science division
Argonne National Laboratory
Lemont, IL 60439
oanam@mcs.anl.gov

October 4, 2024

ABSTRACT

Recently, machine learning tools in particular neural networks have been widely used to solve differential equations. One main advantage of using machine learning, in this case, is that one does not need to mesh the computational domain and can instead randomly draw data points to solve the differential equations of interest. In this work, we propose a simple neural network to approximate low-frequency periodic functions or seek such solutions of differential equations. To this end, we build a Fourier Neural Network (FNN) represented as a shallow neural network (i.e with one hidden layer) based on the Fourier Decomposition. As opposed to traditional neural networks, which feature activation functions such as the sigmoid, logistic, ReLU, hyperbolic tangent and softmax functions, Fourier Neural Networks are composed using sinusoidal activation functions. We propose a strategy to initialize the weights of this FNN and showcase its performance against traditional networks for function approximations and differential equations solutions.

1 Introduction

The last few years have seen revolutionary advances in machine learning techniques in particular through deep learning [7]. The rising availability of data through data collecting initiatives and technologies have made the use of machine learning ubiquitous in fields like image recognition and finance. One popular class of machine learning models is neural networks which were built to mimic the human brain. In the last 60 years, a plethora of neural networks architectures such as Convolutional Neural Networks (CNN) [14], Recurrent Neural Networks (RNN) [10] and autoencoders [24] have been introduced in the literature. Depending on the task to be performed, a specific architecture can prove more advantageous than another one. For function approximation for example, feedforward networks have been widely used [1], [4], [11]. They are multilayered networks where the information travels from the input to the output only in the forward direction. Each layer of a feedforward network is composed of nodes which are linked to the nodes in the previous/next layers through weights and biases and are activated through an activation function e.g the ReLU, logistic, sigmoid functions [18], [8]. The objective of this work is to build a special feedforward network that approximates periodic functions. Periodicity is ubiquitous in nature (periodicity of seasons in climate science etc) and in computational sciences (periodic boundary conditions in large scale applications) and is thus a very relevant computational regime.

In this work, we present a special type of feedforward networks namely Fourier Neural Networks (FNNs) which are shallow neural networks with a sinusoidal activation function. The terminology Fourier Neural

Network stems from the fact that this network tries to mimic the Fourier Decomposition and was first introduced in [26]. However, neural networks with sinusoidal activation functions were first investigated in [6]. In [16], the author presented a FNN which specializes in regression and classification tasks. The authors in [28] provide a comprehensive comparative study between the existing FNN architectures. The main originality of FNNs is the nature of the activation function which incorporates sinusoidal functions and is different from the traditional ones (ReLU, sigmoid function etc). Many approximation theorems have been proved for these traditional activation functions. In [4] and [11] it was proven that shallow neural networks with squashing activation functions such as the logistic or sigmoid functions could approximate any Borel measurable functions to any desired order of accuracy. In [15], it has been proved that multilayered neural networks with nonpolynomial activation function could approximate any function up to $O(1/N)$. In [1], the author gave universal approximation bounds for superpositions of a sigmoidal function for functions whose first moment of the magnitude distribution of the Fourier transform are bounded. When it comes to FNNs, [6] proved an approximation theorem when the activation function is a squashed cosine.

In the first section of this paper, a new methodology to approximate analytic and piecewise analytic periodic functions using FNNs is described and will be used as groundwork to address the second objective of this paper which is seeking periodic solutions to partial differential equations. To that aim, we use the full cosine as an activation function (as opposed to the squashed one). Furthermore, we embed the periodicity information in the loss function which ensures, upon convergence, that the networks will approximate the Fourier series of the function under study. To our knowledge, the FNNs present in the literature [28] were trained according to the Mean Squared Error (MSE) between the desired function and the output of the network. Moreover, we restrict ourselves to the approximation of low-frequency continuous periodic functions. In fact, as shown in [19], a major flaw when training Fourier Neural Networks is that the optimization can stagnate in a local minimum due to the number of oscillations. Limiting ourselves to low-frequency modes and incorporating the periodicity in the loss function effectively allow us to overcome that difficulty. We verify our results with numerical tests and exploit the constructed FNN to accurately recover low-frequency Fourier coefficients of the sought functions. As far as we know, recovering Fourier coefficients using FNNs has never been done in the literature. Additionally, the numerical tests unveiled one tremendous advantage of this new architecture. One bottleneck of Machine Learning is the difficulty of preserving the 'learned' knowledge outside of the training domain. Here, due to the nature of the activation function and of the loss function, the properties learned by the FNN are preserved outside of the training region.

In the second section of this paper, we use the constructed FNN to seek periodic solutions of differential equations. It is intuitive to use the presented FNN to achieve that task as it mimics the Fourier Decomposition of a function. However, to the best of our knowledge, no one has used FNNs to solve differential equations to date. Periodic solutions of differential equations occur naturally, for example, for equations in electronics or oscillatory systems. Some differential equations also have periodic boundary conditions which lead to periodic solutions. Furthermore, there is a growing interest in solving differential equations using neural networks. Authors in [27] introduced the seminal Deep Galerkin Method (DGM) which is a meshfree algorithm that effectively solves high dimensional PDEs by using a deep neural network. Their neural network is trained with a loss function that incorporates the differential equations and the boundary and initial conditions. The DGM algorithm reduces the computational cost of traditional approaches such as the finite difference method by randomly sampling points in the computational domain as opposed to meshing it. In [20] and [21] the authors developed a Physics Informed Neural Network (PINN) that aims at both solving and learning PDEs from data when they are not known. They showcased the performance of their network by effectively solving and learning the Schrödinger, Burgers, Navier-Stokes, Korteweg-de Vries (KdV) and Kuramoto-Sivashinsky equations. A comprehensive discussion on how to solve the Poisson equation and the steady state Navier-Stokes equation based on [20], [21] and [22] is provided in [5]. The authors in [12] modified existing iterative PDEs solvers with a deep neural network in order to accelerate their convergence speed. They train their neural network on a specific geometry and were able to generalize its performance to a more diverse range of boundary conditions and geometries while significantly improving the speedup as compared to the performance of the original solver. Here, we follow [22] and [27] and incorporate the equations in the loss function to obtain a Physics Informed Fourier Neural Network (PIFNN). We show the performance of the built PIFNN on a range of PDEs, such as the Poisson equation and the heat equation.

The rest of this paper is organized as follows: in section 2 we construct the FNN and provide an initialization strategy for the weights and biases of the network. We conclude this section by different numerical simulations that showcase the advantages of the built network. Then, in section 3, we modify the constructed

network so it becomes a Physics Informed Fourier Neural Network (PIFNN) that aims at seeking periodic solutions of a range of differential equations.

2 Fourier Neural Networks as function approximators

A neural network can be seen as a function approximator with a number of inputs M , a number of hidden layers N that are composed of nodes and a number of outputs L . In this work, we focus on shallow neural networks with one input and one output (see figure (1)), the goal being to approximate real valued periodic functions. The output \hat{u} of such neural networks can be written as

$$\hat{u}(x) = \phi_0 + \sum_{k=1}^N \lambda_k \sigma(w_k x + \phi_k), \quad (1)$$

where $x \in \mathbf{R}$ is the input, $w = (w_k, k = 1 \cdots N)$ and $\lambda = (\lambda_k, k = 1 \cdots N)$ are the weights of the neural network, σ the activation function, and $\phi = (\phi_k, k = 0 \cdots N)$ its biases.

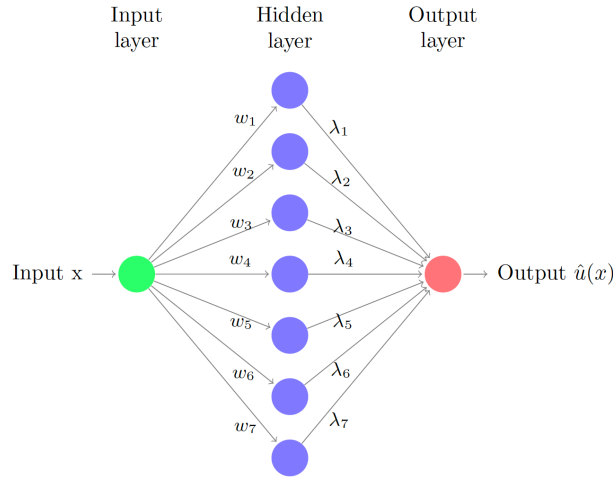


Figure 1: Fully connected neural network with a single hidden layer and a one-dimensional input $x \in \mathbf{R}$

On the other end, the Fourier series representation $S_N u$ of a T -periodic function $u \in L^2(\mathbf{R})$ is

$$S_N u(x) = \frac{a_0}{2} + \sum_{n=1}^N a_n \cos(n\omega x) + b_n \sin(n\omega x) \quad (2)$$

where $x \in [-\frac{T}{2}, \frac{T}{2}]$, $\omega = \frac{2\pi}{T}$ and a_n and b_n are the Fourier coefficients of u . It can be rewritten in the following reduced (phase shift) form:

$$S_N u(x) = \frac{a_0}{2} + \sum_{n=1}^N c_n \cos(n\omega x + \psi_n) \quad (3)$$

where for $n \geq 1$, $c_n = \sqrt{a_n^2 + b_n^2}$ and $\psi_n = \arctan 2(-\frac{b_n}{a_n})$.

Therefore, by taking the activation function to be the function $x \mapsto \cos(\omega x)$ in equation (1), one obtains a formulation that resembles the Fourier decomposition. The input to hidden layer weights w_k mimic the nodes n , the hidden layer to output weights λ_k approximate the Fourier coefficients c_n , the biases of the hidden layer ϕ_k correspond to the phase shifts ψ_k and the bias of the output ϕ_0 to half the 0th order Fourier coefficient a_0 . However as we empirically show below, the equivalency is not straightforward and one needs to train the network with a specific loss function in order to obtain satisfactory results. In the rest of this paper, we restrict ourselves to 2-periodic function which means the activation function is $x \mapsto \cos(\pi x)$.

2.1 Loss function

The goal of our network is to approximate the Fourier series $S_N u$ of u . To that end, we define the loss function as

$$L(\phi, w, \lambda) = \|\hat{u} - u\|_2^2 + \alpha_1 \|\lambda\|^2 + \alpha_2 \|w\|^2 \quad (4)$$

where

1. The first term $\|\hat{u} - u\|_2^2$ ensures that the output of the neural network approximates the target function u ,
2. The second $\alpha_1 \|\lambda\|^2$ and third $\alpha_2 \|w\|^2$ terms are regularization terms to avoid overfitting of the Neural Network. Choosing a L^2 norm for the regularization parameters causes the weights to decay asymptotically to zero, while a L^1 regularization might decrease them to exactly zero. We reserve the choice of the regularization norm for section 2.3.

However, this loss function will not provide an approximation of the Fourier series of a function unless that function is an exact combination of cosines or sines. For example, fitting $u(x) = x^2$ with one neuron in the hidden layer led to the output

$$\hat{u}(x) = \phi_0 - \lambda_1 \cos(\pi w_1 x)$$

where $\frac{\lambda_1 \pi^2 w_1^2}{2!} \approx 1$, $\lambda_1 \approx \phi_0 \approx 1$ and $(\pi w_1)^{2l} \ll 1$ for $l > 1$. While this, using the fact that

$$\cos(\pi w_1 x) = \sum_{l=1}^{\infty} (-1)^l \frac{(\pi w_1)^{2l} x^{2l}}{(2l)!} = 1 - \frac{\pi^2 w_1^2}{2!} x^2 + o(w_1^3)$$

or equivalently

$$x^2 \approx (1 - \cos(\pi w_1 x)) \frac{2!}{\pi^2 w_1^2} \approx \phi_0 - \lambda_1 \cos(\pi w_1 x)$$

is a good approximation of x^2 , is not the desired output. To obtain the Fourier representations of the target functions, the weights from the input to the hidden layer need to be approximately integers. This can be achieved by solving a mixed integer optimization problem which is out of the scope of this paper or by modifying the loss function as follows

$$L(\phi, w, \lambda) = \|\hat{u}(x) - u(x)\|_2^2 + \alpha_1 \|\lambda\|^2 + \alpha_2 \|w\|^2 + \alpha_3 (\|\hat{u}(x+T) - \hat{u}(x)\|_2^2) + \alpha_4 (\|\hat{u}(x-T) - \hat{u}(x)\|_2^2) \quad (5)$$

This amounts to forcing the output of the neural network to be periodic and is equivalent to the input to hidden layer weights being approximately integers.

2.2 Weights and biases initialization

A proper weight initialization can significantly improve the performance of a neural network in the training phase specially when dealing with Deep Neural Networks (DNN). In fact, when training a DNN, one is often faced with the vanishing/exploding gradients phenomenon [7] which causes the training to not converge to a good solution. The authors in [8] have proposed an initialization method when using the logistic activation function that circumvent the vanishing/exploding gradients issue. In essence, they proved that one needs the variance of the outputs of each layer to be equal to the variances of its inputs. Furthermore, the variances of the gradients should be equal before and after going through a layer in the reverse direction. [9] proposed an initialization strategy for the ReLU activation function. In [13], the author extended this result to nonlinear activation functions differentiable at 0. Even though we are considering a shallow neural network in this work, initialization is important to speed up the training and we propose below an initialization strategy for the FNN presented here. As it is commonly the case, we initialize the biases to 0. In what follows, we use a few properties of the mean and variance of a random variable that are recalled in appendix A and we denote by X a random variable to differentiate it from its realization x .

Let x be the input of our FNN and $\{x_k\}_{k=1..N}$ the hidden layer nodes (see figure 1). For the sake of simplicity, we denote by y the output of the network instead of $\hat{u}(x)$ in this section. . Then, as the biases are equal to 0,

$$x_k = \cos(\pi w_k x) \text{ and } y = \sum_{k=1}^N \lambda_k \cos(\pi w_k x).$$

We assume that the input x of the FNN is a vector of size M whose elements were drawn uniformly in $[-1 \ 1]$. That means (see appendix A) that

$$\mu(X) = 0 \text{ and } \sigma^2(X) = \frac{1}{3}.$$

where $\mu(X)$ denotes the mean of a random variable X and $\sigma^2(X)$ its variance defined by

$$\begin{aligned} \mu(X) &= \int_{-\infty}^{+\infty} xf(x)dx \\ \sigma^2(X) &= \mu(X^2) - (\mu(X))^2 \end{aligned}$$

Furthermore, we assume the weights w_k are drawn from a normal distribution $\mathcal{N}(0, m^2)$ and the weights λ_k are drawn from a normal distribution $\mathcal{N}(0, v^2)$. The goal is to find values of m and v such that the variances at each of the layers of the network are equal during the first forward pass i.e

$$\sigma^2(X) = \sigma^2(X_k) = \sigma^2(Y), \quad \forall k = 1 \cdots N$$

Initializing the input layer to hidden layer weights w_k : We first compute the mean of the node k of the hidden layer. To that aim, we use the following theorem called the Law Of The Unconscious Statistician (LOTUS).

Theorem 1. *Let X, Y be continuous random variables with a joint density function $f_{(X,Y)}$ and h be a continuous function of two variables such that*

$$\begin{aligned} \int_{\mathbf{R}^2} |h(x, y)| f_{(X,Y)}(x, y) dx dy &< +\infty, \text{ then, we have} \\ \mu(h(X, Y)) &= \int_{\mathbf{R}^2} h(x, y) f_{(X,Y)}(x, y) dx dy \end{aligned}$$

Therefore, knowing that the joint probability distribution of the two independent random variables W_k and X is

$$f_{(W_k, X)}(x, y) = \frac{1}{2} \cdot \frac{1}{m\sqrt{2\pi}} e^{-\frac{w_k^2}{2m^2}},$$

we obtain (using $h(w_k, x) = \cos(\pi w_k x)$ in the above theorem)

$$\mu(X_k) = \mu(\cos(\pi W_k X)) = \int_{-1}^1 \int_{-\infty}^{+\infty} \frac{1}{2} \cos(\pi w_k x) \frac{1}{m\sqrt{2\pi}} e^{-\frac{w_k^2}{2m^2}} dw_k dx. \quad (6)$$

Let $I_1(x) = \int_{-\infty}^{+\infty} \cos(\pi w_k x) \frac{1}{m\sqrt{2\pi}} e^{-\frac{w_k^2}{2m^2}} dw_k$. We can differentiate under the integral sign to obtain

$$I_1'(x) = - \int_{-\infty}^{+\infty} \pi w_k \sin(\pi w_k x) \frac{1}{m\sqrt{2\pi}} e^{-\frac{w_k^2}{2m^2}} dw_k.$$

After integrating by parts $I_1'(x)$, we find I_1 satisfies the differential equation

$$I_1'(x) + \pi^2 m^2 x I_1(x) = 0, \quad I_1(0) = \int_{-\infty}^{+\infty} \frac{1}{m\sqrt{2\pi}} e^{-\frac{w_k^2}{2m^2}} dw_k = \frac{m}{|m|}$$

which admits the unique solution

$$I_1(x) = \frac{m}{|m|} e^{-\frac{1}{2}\pi^2 m^2 x^2} = e^{-\frac{1}{2}\pi^2 m^2 x^2}.$$

This means

$$\mu(X_k) = \int_{-1}^1 \frac{1}{2} e^{-\frac{1}{2}\pi^2 m^2 x^2} dx$$

which, after integration, gives

$$\mu(X_k) = \frac{1}{m\sqrt{2\pi}} \operatorname{erf}\left(\frac{m\pi}{\sqrt{2}}\right) \quad (7)$$

where erf is the error function.

Now, to compute the variance of X_k , we recall that

$$\sigma^2(X_k) = \mu(X_k^2) - (\mu(X_k))^2.$$

We then use the trigonometric identity

$$x_k^2 = \cos^2(\pi w_k x) = \frac{1}{2} + \frac{\cos(2\pi w_k x)}{2}$$

which leads to

$$\mu(X_k^2) = \int_{-1}^1 \frac{1}{2} \int_{-\infty}^{+\infty} \frac{1}{2} (1 + \cos(2\pi w_k x)) \frac{1}{m\sqrt{2\pi}} e^{-\frac{w_k^2}{2m^2}} dw_k dx$$

After integration, we obtain

$$\mu(X_k^2) = \frac{1}{2} + \frac{1}{4\sqrt{2\pi}} \frac{erf(\sqrt{2}m\pi)}{m}.$$

Put together, the variance of X_k becomes

$$\sigma^2(X_k) = \frac{1}{2} + \frac{1}{4\sqrt{2\pi}} \frac{erf(\sqrt{2}m\pi)}{m} - \left(\frac{1}{m\sqrt{2\pi}} erf\left(\frac{m\pi}{\sqrt{2}}\right) \right)^2. \quad (8)$$

Because we want the variance of the output of the hidden layer to be equal to the variance of its input i.e

$$\sigma^2(X_k) = \sigma^2(X) = \frac{1}{3},$$

we need to solve

$$\frac{1}{3} = \frac{1}{2} + \frac{1}{4\sqrt{2\pi}} \frac{erf(\sqrt{2}m\pi)}{m} - \left(\frac{1}{m\sqrt{2\pi}} erf\left(\frac{m\pi}{\sqrt{2}}\right) \right)^2.$$

which admits a unique solution $m \approx 0.6959$. However, this value being small, this means that imposing this type of initialization on the hidden layer weights will cause the FNN to capture fewer Fourier modes than we are seeking. Therefore, we initialize these weights using a normal distribution $\mathcal{N}(0, 5)$ which means $m = \sqrt{5}$. This value was picked by trial and error and as showed in the results section 2.3, allows us to recover the first five Fourier coefficients of a periodic function. Plugging in m in equation (8) gives

$$\sigma^2(X_k) \approx .5128$$

Initializing the hidden layer to output layer weights λ_k : Now, for the output y , since Λ_k and $\cos(W_k X)$ are independent, we can write

$$\mu(Y) = \sum_{k=1}^N \mu(\lambda_k) \mu(\cos(w_k x))$$

and

$$\sigma^2(Y) = \sum_{k=1}^N \sigma^2(\Lambda_k) (\sigma^2(\cos(W_k X)) + \mu^2(\cos(W_k X))) + \mu^2(\Lambda_k) \sigma^2(\cos(W_k X))$$

where $\sigma^2(\Lambda_k) = v^2$ and $\mu(\Lambda_k) = 0$. This leads to

$$\sigma^2(Y) = N \left[v^2 \left[\frac{1}{2} + \frac{1}{4\sqrt{2\pi}} \frac{erf(\sqrt{2}m\pi)}{m} \right] \right]. \quad (9)$$

Since we want $\sigma^2(Y) = \sigma^2(X_k) \approx .5128$, we get

$$v^2 = \frac{0.5128}{N \left(\frac{1}{2} + \frac{1}{4\sqrt{2\pi}} \frac{erf(\sqrt{2}m\pi)}{m} \right)} \quad (10)$$

where $m = \sqrt{5}$.

2.3 Results

In this section, we run numerical simulations to assess the effectiveness of the method presented above. We first approximate analytic 2-periodic functions which are linear combinations of sines and cosines. High accuracy is expected on such functions due to the way the FNN was built. Then, we aim at recovering low-frequency Fourier coefficients of piecewise analytic periodic functions. These functions are of particular interest since they are very common in fields like acoustics or electronics.

2.3.1 Analytic Periodic Functions

In order to investigate the performance of the above constructed network, we first attempt to approximate the 2-periodic function

$$f(x) = \cos(\pi x) + \sin(\pi x) .$$

with four nodes in the hidden layer. We show results for both L^2 and L^1 regularizations. We report the parameters of the network upon convergence in tables (1-2) along with the number of iterations and the value loss function. We notice that the output of the FNN is

$$\hat{u}(x) \approx \sqrt{2} \cos(\pi x - \frac{\pi}{4})$$

which is the reduced form of $f(x) = \cos(\pi x) + \sin(\pi x)$. The optimization converged to approximately $2e - 4$ in 189 iterations for the L^2 regularization against $3e - 4$ in 87 iterations for the L^1 one. Although the results for the L^1 regularization are slightly better, none of the hidden layer to output weights converged to exactly zero as was expected.

Number of iterations			189
Loss Function (upon convergence)			$2e - 4$
w_k	ϕ_k	λ_k	ϕ_0
1.00000000	$-0.78539816 \approx -\pi/4$	$1.41421354 \approx \sqrt{2}$	$-1.81893539e - 05$
$-5.96856597e - 07$	-1.00911547	$-2.60499122e - 05$	
$1.22755482e - 06$	1.87773726	$-4.76966579e - 05$	
$4.59348246e - 08$	-6.38405893	$1.77429347e - 05$	

Table 1: Number of iterations, value of the loss function at convergence and optimal weights and biases of the FNN to approximate $f(x) = \cos(\pi x) + \sin(\pi x)$, $k = 1 \dots 4$ with a L^2 regularization.

Number of iterations			87
Loss Function (upon convergence)			$3e - 4$
w_k	ϕ_k	λ_k	ϕ_0
1.00000033	$-0.78540193 \approx -\pi/4$	$1.41421847 \approx \sqrt{2}$	$1.58219741e - 05$
1.4969094	-0.71483098	$-4.32639025e - 06$	
0.05095418	0.96613253	$6.73308554e - 05$	
0.14126515	-5.84166681	$-5.13186621e - 05$	

Table 2: Number of iterations, value of the loss function at convergence and optimal weights and biases of the FNN to approximate $f(x) = \cos(\pi x) + \sin(\pi x)$, $k = 1 \dots 4$ with a L^1 regularization.

We compare in figure (2) the performances of the above constructed FNN and of a regular neural network with a \tanh activation function and a Glorot initialization [8]. The latter network converged to approximately $1e - 3$ in 1173 iterations which showcases the significant gain in iteration number obtained when using the FNN. The error is also improved by an order of 10 with the FNN. To further illustrate the advantages of using the presented FNN, we display in figure (3) a significant benefit it has. In fact, it also produces a good approximation of the desired function outside of the training domain. A major shortcoming of neural networks methods for function approximation is indeed their inability to preserve the sought function outside of the training region. The architecture presented here is able to overcome that issue due to the way the loss function was defined in equation (5). It is worth noting that we did not include the periodicity requirement in

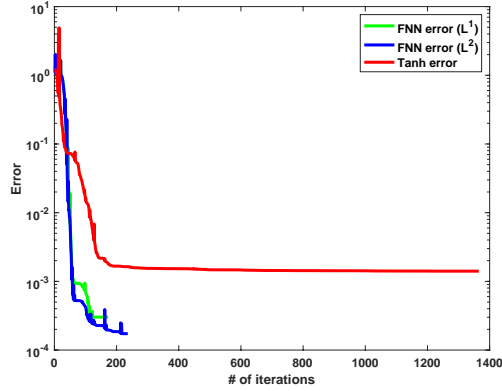


Figure 2: Comparison in terms of the values of the loss function throughout the optimization when using a FNN and when using a neural network with a tanh activation.

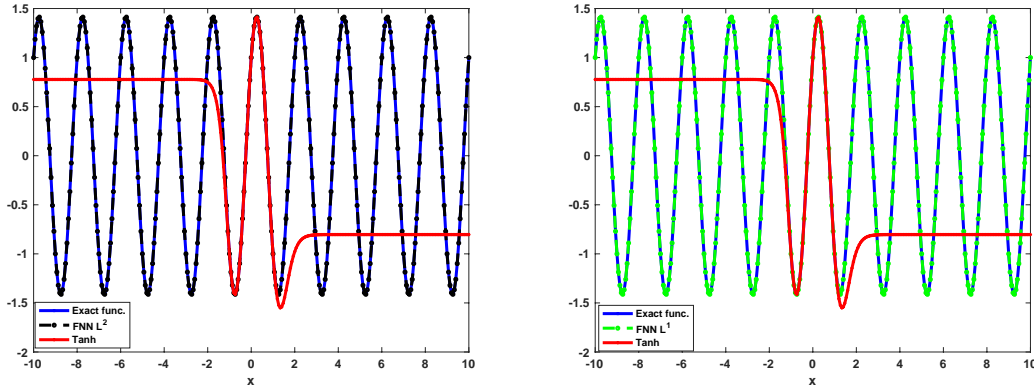


Figure 3: Comparison between $f(x) = \cos(\pi x) + \sin(\pi x)$ and the output of the FNN outside of the training domain for both L^2 (left) and L^1 (right) regularizations

the loss function when training the traditional neural network, the results were worst in that it required more nodes in the hidden layer, convergence was reached more slowly and the error was similar.

We then seek to estimate the function

$$g(x) = 8 \cos(4\pi x) + \sin(2\pi x) + \sin(\pi x)$$

with the same architecture as above. We show in tables (3-4) the value of the loss function (error) upon convergence, the number of iterations as well as the values of the weights obtained upon convergence. The optimization converged to approximately $9e - 4$ after 195 iterations when using a L^2 regularization on the weights and to approximately $1e - 3$ after 169 iterations when using a L^1 one. We note the biases are approximations of odd multiples of $\pi/2$ for the sine part of the function g and approximately 0 for its cosine part.

We show in figure (4) a comparison between the exact function g and the approximations provided by the FNN. The actual error between the function and the FNN approximation only is of the order of $1e - 8$ for the L^2 regularization and $1e - 5$ for the L^1 one. This, combined with the fact that weights corresponding to redundant node don't go exactly to zero when using L^1 regularization, motivates us to use L^2 regularization in the rest of the paper. We also compared the FNN approximation to one from a regular neural network with a tanh activation. The latter converged to a poor local minimum for 4 nodes in the hidden layer and converged to a value of $3e - 2$ for the loss function for 10 nodes in the hidden layer.

Number of iterations			195
Loss Function (upon convergence)			$9e - 4$
w_k	ϕ_k	λ_k	ϕ_0
1.00000000	$1.57079627 \approx \pi/2$	$-9.99999993e - 01$	$2.41330937e - 06$
$5.40604942e - 06$	$1.01888743e + 01$	$3.34351764e - 06$	
4.00000000	$-9.14402304e - 10$	7.99999983	
-2.00000000	$4.71238899 \approx 3\pi/2$	$-9.99999984e - 01$	

Table 3: Number of iterations, value of the loss function at convergence and optimal weights and biases of the FNN to approximate $g(x) = 8 \cos(4\pi x) + \sin(2\pi x) + \sin(\pi x)$ with L^2 regularization, $k = 1 \dots 4$

Number of iterations			169
Loss Function (upon convergence)			$1e - 3$
w_k	ϕ_k	λ_k	ϕ_0
0.99999306	$1.57072838 \approx \pi/2$	-1.000141261	$3.82384745e - 05$
1.99999672	$7.85406634 \approx 5\pi/2$	$-9.99825909e - 01$	
3.99999998	$-1.14376588e - 05$	7.99989569	
-0.04032155	$-2.12089270e + 01$	$1.69927207e - 05$	

Table 4: Number of iterations, value of the loss function at convergence and optimal weights and biases of the FNN to approximate $g(x) = 8 \cos(4\pi x) + \sin(2\pi x) + \sin(\pi x)$ with L^1 regularization, $k = 1 \dots 4$

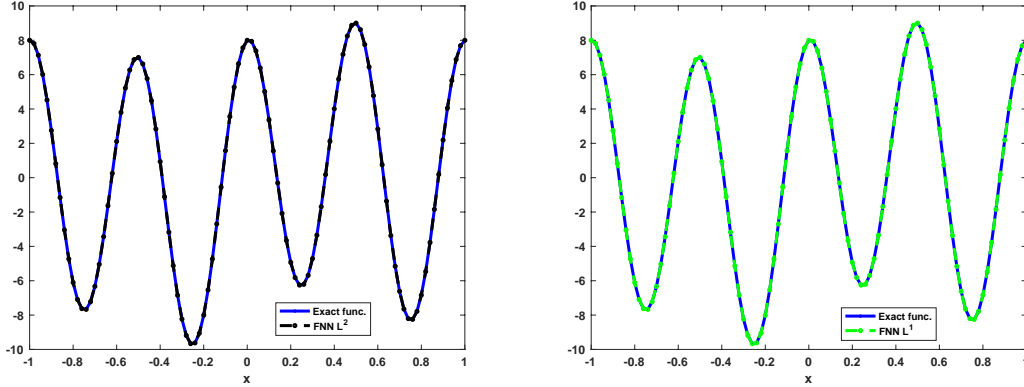


Figure 4: Comparison between $g(x) = 8 \cos(4\pi x) + \sin(2\pi x) + \sin(\pi x)$ and the output of the FNN for both L^2 (left) and L^1 (right) regularizations

2.3.2 Piecewise analytic periodic functions

Here, we first tried to approximate the non analytical periodic function

$$f(x) = x^2, \quad x \in (-(2k+1), (2k+1)) \quad , k \in \mathbb{N} \quad (11)$$

We use 4 nodes in the hidden layer and the FNN captured the first five nodes of the Fourier decomposition (if we count the 0th node). We show in table (5) the values obtained for the weights and the biases. We call the hidden layer to output weights and the bias of the output layer FNN coefficients. We note that they are 3rd order approximations of the Fourier coefficients. Figure (5) is a good visual representation of the quality of that approximation. The Fourier series of this function is

$$S(f)(x) = \frac{1}{3} + \sum_{n=1}^{\infty} 4 \frac{(-1)^n}{\pi^2 n^2} \cos(\pi n x)$$

Number of iterations			130
Loss Function (upon convergence)			$2e - 2$
w_k	ϕ_k	λ_k	ϕ_0
0.99995578	-0.00477923	-0.40479907	0.335023246
2.99892898	-3.139197051	0.04915202	
3.99604127	0.01794715	0.02874206	
-1.99965386	0.00445702	0.10497063	

Table 5: Number of iterations, value of the loss function at convergence and optimal weights and biases of the FNN to approximate $f(x) = x^2$ on $[-1, 1]$

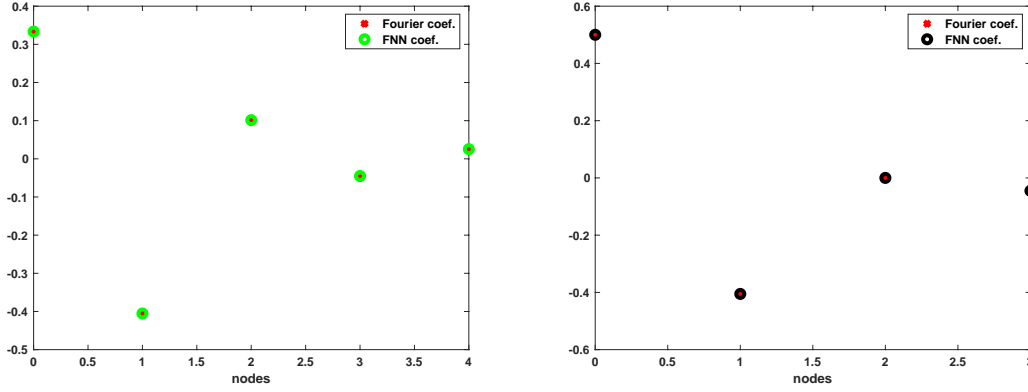


Figure 5: Comparison between the FNN coefficients and the Fourier coefficients of $f(x) = x^2$ (left) and of $g(x) = |x|$ (right) for the nodes captured by the neural network

We illustrate in figure (6) the behavior of the output of the FNN as opposed to the one from a neural network with a \tanh activation function. As expected, the FNN network conserves the properties of the function to be approximated outside of the training domain while the \tanh neural network does not. It is worth noting that the latter was more accurate in this case on the training interval $[-1, 1]$ ($6e - 4$ with 3073 iterations against $2e - 2$ with 130 iterations for the FNN.)

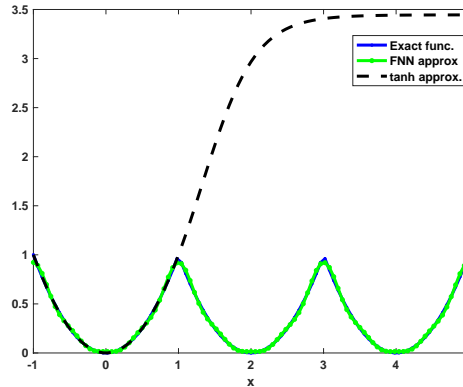


Figure 6: Comparison between the FNN and the \tanh approximations outside the training domain for $f(x) = x^2$

To conclude the numerical tests in this section, we approximate the function

$$g(x) = |x|, \quad x \in (-(2k+1), (2k+1)) \quad , k \in \mathbb{N} \quad (12)$$

The Fourier series of this function is

$$S(g)(x) = \frac{1}{2} + \sum_{n=1}^{\infty} -4 \frac{(1)}{\pi^2(2n-1)} \cos(\pi(2n-1)x)$$

We summarize the FNN coefficients in table (6) as well as the biases produced by the FNN. The FNN was able to capture the first 4 nodes of the Fourier decomposition. This can be explained by the fact g only admits Fourier coefficients for odd coefficients. As before, we provide in figure (5) (right) a visual representation to compare the Fourier coefficients of g to its FNN coefficients. Similar results to those obtained for the function f (11) are observed here. The FNN coefficients are good approximations of their Fourier counterparts and the error between the two is of the 3rd order.

Number of iterations			445
Loss Function (upon convergence)			$1e-2$
w_k	ϕ_k	λ_k	ϕ_0
0.99995402	$-2.44738021e-03$	-0.40420162	0.502531
2.98845687	$-1.68031025e-01$	0.03295792	
2.99445216	$-6.78306499e-02$	-0.07711458	
-1.99075052	-9.45244148	-0.00391551	

Table 6: Number of iterations, value of the loss function at convergence and optimal weights and biases of the FNN to approximate $f(x) = |x|$ on $[-1, 1]$

3 Fourier neural networks as differential equations solvers

The use of Machine Learning (ML) in the field of differential equations has raised considerable and widespread interest in recent years. ML techniques have been used to effectively solve differential equations [5], [12], [21], [22], and [27] but also to discover underlying dynamics from data [2], [20] and [23] and even to build robust neural networks architectures based on differential equations [3], [17] and [25]. In this section, we extend the work presented in section 2 to seek periodic solutions of differential equations of the type

$$Pu = f$$

where P is a differential operator. To that aim, we follow [20] and [27] and use the loss function

$$L(\phi, w, \lambda) = \|P\hat{u}(x) - f(x)\|_2^2 + \alpha_2 \|\lambda\|_2^2 + \alpha_3 \|w\|_2^2 + \alpha_3 (\|\hat{u}(x+T) - \hat{u}(x)\|_2^2) + \alpha_4 (\|\hat{u}(x-T) - \hat{u}(x)\|_2^2) \quad (13)$$

that incorporates the physics into the loss function to obtain what we call a Physics Informed Fourier Neural Network (PIFNN). This name is inspired by the one introduced in [22]. We illustrate the performance of the PIFNN by solving the one-dimensional Poisson and heat equations.

3.1 Poisson equation

w_k	ϕ_k	λ_k	ϕ_0
$-3.77424453e-10$	-4.42730681	$4.90842033e-05$	0
$-1.16548318e-10$	2.46210794	$-1.45660922e-05$	
1.00000000	$3.14159265 \approx \pi$	$-1.01321184e-01 \approx -1/\pi^2$	
$-1.18183192e-09$	0.79153364	$-1.60990031e-06$	

Table 7: Optimal weights and biases of the FNN to solve the Poisson equation (14), $k = 1 \dots 4$

First, we solve the Poisson equation

$$-\Delta u = \cos(\pi x), \quad x \in [-1, 1]. \quad (14)$$

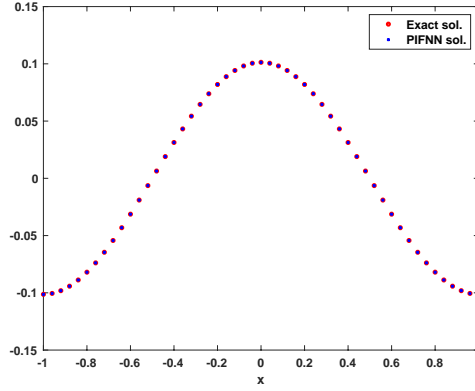


Figure 7: Comparison between the PIFNN and the exact solutions

with the constructed PIFNN. To assess the quality of the PIFNN solution, we compare it to the exact solution of this equation which is given by $u = \frac{1}{\pi^2} \cos(\pi x)$. We show both solutions in figure (7) and we report the weights and biases of the PIFNN in table (7). We note that the output is

$$\hat{u}(x) = -\frac{1}{\pi^2} \cos(\pi x + \pi) + o(1e-5) \approx \frac{1}{\pi^2} \cos(\pi x).$$

which is a 5th order approximation of the exact solution. We obtain an additional advantage of the PIFNN when seeking periodic solutions of the Poisson equation. In fact, it produces a closed formula for this equation and the exact one can be retrieved from it.

3.2 Heat equation

Here, we solve the heat equation

$$\begin{aligned} \frac{\partial u}{\partial t} &= \frac{\partial^2 u}{\partial x^2}, & x \in [-1, 1], \quad t \in [0, 4] \\ u(0, x) &= u_0(x) = \sin(\pi x), \\ u(t, -1) &= u(t, 1). \end{aligned} \tag{15}$$

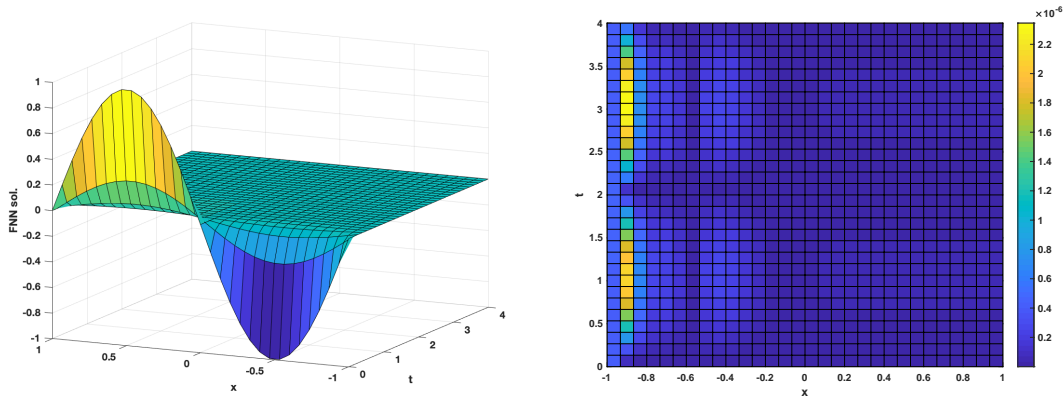


Figure 8: Solution produced by the PIFNN for the heat equation (left) and error from the exact solution (right)

To account for the time dependency, we rewrite the heat equation using the separation of variables method. To this end, we set $u(x, t) = X(x)T(t)$ which transforms the equation into

$$X(x)T'(t) = X''(x)T(t).$$

We rewrite the cost function as follows

$$\begin{aligned}
L(\phi, w, \lambda) = & \alpha_1 ||\hat{X}(x)\hat{T}'(t) - \hat{X}''(x)\hat{T}(t)||^2 \\
& + \alpha_2 ||\lambda||^2 + \alpha_3 ||w||^2 \\
& + \alpha_3 ||\hat{X}(x+2) - \hat{X}(x)||^2 \\
& + \alpha_4 ||\hat{X}(x-2) - \hat{X}(x)||^2 \\
& + \alpha_5 ||\hat{T}_0(x) - \hat{u}_0(x)||^2
\end{aligned}$$

to incorporate the boundary and initial conditions and separate the network into two independent subnetworks. The first with the PIFNN architecture that deals with the space dependent function X and second with a regular architecture (with a \tanh activation function) that works on the time dependent function T . The left part of figure (8) corresponds the solution produced by the PIFNN and the right part shows the error between that solution and the exact one which is $u(x) = \sin(\pi x)e^{-\pi^2 t}$, $t \in [0, 4]$. We note from figure (8) that the error between the two is of order 6.

4 Conclusion

We have constructed a novel Fourier Neural Network (FNN) architecture that successfully approximates low-frequency analytic and piecewise analytic one dimensional periodic functions. We were able to retrieve the Fourier coefficients for such functions with third order accuracy. We also showed how to seek periodic solutions for simple one dimensional differential equations. These results were achieved by imposing periodicity constraints to the optimization problem we are solving and by subsequently solving the problem with a penalty-like method. Besides significantly improving the results obtained using traditional neural networks in terms of accuracy and number of iterations, our simulations revealed another important advantage, namely, it conserves the properties of the learned task (approximating a function etc) outside of the training domain. One limitation of our model is that we are not using a rigorous technique for picking the penalty coefficients but are instead setting them up by trial and error. Another limitation is that we need to know the periodicity of the function we are estimating a priori in order to incorporate it in the activation function. We are currently in the process of investigating solutions to overcome these limitations. Our results are promising and we are planning on extending to multidimensional functions in future work. We believe the framework presented here can serve as a preprocessing tool for many engineering and scientific applications such as electronics, image recognition and acoustics where the Fourier decomposition is widely used.

Acknowledgement

The authors would like to thank Charlotte Haley for her pertinent suggestions. This material is based upon work supported by the U.S. Department of Energy, Office of Science, Advanced Scientific Computing Research under Contract DE-AC02-06CH11357.

Government License. The submitted manuscript has been created by UChicago Argonne, LLC, Operator of Argonne National Laboratory ("Argonne"). Argonne, a U.S. Department of Energy Office of Science laboratory, is operated under Contract No. DE-AC02-06CH11357. The U.S. Government retains for itself, and others acting on its behalf, a paid-up nonexclusive, irrevocable worldwide license in said article to reproduce, prepare derivative works, distribute copies to the public, and perform publicly and display publicly, by or on behalf of the Government. The Department of Energy will provide public access to these results of federally sponsored research in accordance with the DOE Public Access Plan. <http://energy.gov/downloads/doe-public-access-plan>.

A Some statistical properties

We recall below some properties verified by the mean μ and the variance σ^2 of a random variable.

1. $\mu(aX + Y) = a\mu(X) + \mu(Y)$ and $\sigma^2(aX + Y) = a^2\sigma^2(X) + \sigma^2(Y)$ where $a \in \mathbf{R}$, and X and Y are two random variables.

2. $\mu(XY) = \mu(X)\mu(Y)$ and $\sigma^2(XY) = \sigma^2(X)(\mu^2(Y) + \sigma^2(Y)) + \mu^2(X)\sigma^2(Y)$ where X and Y are two independent random variables.

We also recall the value of the mean and of the variance of the two distributions used in the paper i.e the uniform and normal distributions.

1. If $X \sim \mathcal{U}([a, b])$ then:

- $\mu(X) = \frac{1}{b-a}$ and $\sigma^2(X) = \frac{(b-a)^2}{12}$,
- The probability density function (pdf) of X is $f_X(x) = 1/(b-a)$ if $x \in [a, b]$ and 0 otherwise.

2. If $X \sim \mathcal{N}(0, m^2)$ then:

- $\mu(X) = 0$ and $\sigma^2(X) = m^2$,
- The probability density function (pdf) of X is $f_X(x) = \frac{1}{\sigma\sqrt{2\pi}} e^{-\frac{x^2}{2\sigma^2}}$.

References

- [1] Andrew Barron. Universal approximation bounds for superpositions of a sigmoidal function. *Machine learning and cybernetics*, 1993.
- [2] Steven L. Brunton, Joshua L. Proctor, and Nathan Kutz. Discovering governing equations from data by sparse identification of nonlinear dynamical systems. *Proceedings of the National Academy of Sciences of the United States of America*, 2016.
- [3] Tian Qi Chen, Yulia Rubanova, Jesse Bettencourt, and David Duvenaud. Neural ordinary differential equations. *32nd Conference on Neural Information Processing Systems*, 2018.
- [4] George Cybenko. Approximation by superpositions of a sigmoidal function. *Mathematics of Control, Signals and Systems*, 1992.
- [5] Tim Dockhorn. A discussion on solving partial differential equations using neural networks. 2019.
- [6] Ronald Gallant and Halbert White. There exists a neural network that does not make avoidable mistakes. *Proceedings of the second annual IEEE conference on neural networks*, 1988.
- [7] Aurelien Geron. *Hands-On Machine Learning with Scikit-Learn and TensorFlow*. O'Reilly Media, Inc., 2017.
- [8] Xavier Glorot and Yoshua Bengio. Understanding the difficulty of training deep feedforward neural networks. *Neural Networks*, 2010.
- [9] Kaiming He, Xiangyu Zhang, Shaoqing Ren, and Jian Sun. Delving deep into rectifiers: Surpassing human-level performance on imagenet classification. *Proceedings of the 2015 IEEE International Conference on Computer Vision*, 2015.
- [10] Sepp Hochreiter and Juergen Schmidhuber. Long short-term memory. *Parallel Distributed Processing*, 1986.
- [11] Kurk Hornik, Maxwell Stinchcombe, and Halbert White. Multilayer feedforward networks are universal approximators. *Neural Networks*, 1989.
- [12] Jun-Ting Hsieh, Shengjia Zhao, Stephan Eismann, Lucia Mirabella, and Stefano Ermon. Learning neural pde solvers with convergence guarantees. *International Conference on Learning Representations 2019*, 2019.
- [13] Siddharth K. Kumar. On weight initialization in deep neural networks. 2017.
- [14] Yann LeCun, Patrick Haffner, Léon Bottou, and Yoshua Bengio. Object recognition with gradient-based learning. *International Workshop on Shape, Contour and Grouping in Computer Vision*, 1999.
- [15] Moshe Leshno, Vladimir Lin, Allan Pinkus, and Shimon Schocken. Multilayer feedforward networks with a nonpolynomial activation function can approximate any function. *Neural Networks*, 1993.
- [16] Shuang Liu. Fourier neural network for machine learning. *2013 International Conference on Machine Learning and Cybernetics*, 2013.
- [17] Zichao Long, Yiping Lu, Xianzhong Ma, and Bin Dong. Pde-net: Learning pdes from data. *Proceedings of the 35th International Conference on Machine Learning*, 2019.

- [18] Chigozie Nwankpa, Winifred Ijomah, Anthony Gachagan, and Stephen Marshall. Activation functions: Comparison of trends in practice and research for deep learning. 2018.
- [19] Giambattista Parascandolo, Heikki Huttunen, and Tuomas Virtanen. Taming the waves: sine as activation function in deep neural networks. 2017.
- [20] Maziar Raissi. Deep hidden physics models: Deep learning of nonlinear partial differential equations. *Journal of Machine Learning Research*, 2018.
- [21] Maziar Raissi and George Em Karniadakis. Hidden physics models: Machine learning of nonlinear partial differential equations. *Journal of Computational Physics*, 2017.
- [22] Maziar Raissi, Paris Perdikaris, and George Em Karniadakis. Physics-informed neural networks: A deep learning framework for solving forward and inverse problems involving nonlinear partial differential equations. *Journal of Computational Physics*, 2019.
- [23] Samuel H. Rudy, Steven L. Brunton, Joshua L. Proctor, and Nathan Kutz. Data-driven discovery of partial differential equations. *Science Advances*, 2017.
- [24] David E. Rumelhart, Geoffrey E. Hinton, and Ronald J. Williams. Learning internal representations by error propagation. *Neural computation*, 1997.
- [25] Lars Ruthotto and Eldad Haber. Deep neural networks motivated by partial differential equations. *Journal of Mathematical Imaging and Vision volume*, 2019.
- [26] Adrian Silvescu. Fourier neural networks. *International joint conference on neural networks*, 1999.
- [27] Justin Sirignano and Konstantinos Spiliopoulos. Dgm: A deep learning algorithm for solving partial differential equations. *Journal of Computational Physics*, 2018.
- [28] Abylay Zhumekenov, Malika Uteuliyeva, Olzhas Kabdolov, Rustem Takhanov, Zhenisbek Assylbekov, and Alejandro J. Castro. Fourier neural networks: A comparative study. 2019.